

Stochastic Analysis of WPT Efficiency due to Location Uncertainty of mm-Sized Deep-Implanted Pacemakers

Icaro V. Soares, Denys Nikolayev

▶ **To cite this version:**

Icaro V. Soares, Denys Nikolayev. Stochastic Analysis of WPT Efficiency due to Location Uncertainty of mm-Sized Deep-Implanted Pacemakers. 2022 Wireless Power Week (WPW), Jul 2022, Bordeaaux, France. hal-03827227v1

HAL Id: hal-03827227

https://hal.science/hal-03827227v1

Submitted on 11 Nov 2023 (v1), last revised 25 Nov 2022 (v2)

HAL is a multi-disciplinary open access archive for the deposit and dissemination of scientific research documents, whether they are published or not. The documents may come from teaching and research institutions in France or abroad, or from public or private research centers.

L'archive ouverte pluridisciplinaire **HAL**, est destinée au dépôt et à la diffusion de documents scientifiques de niveau recherche, publiés ou non, émanant des établissements d'enseignement et de recherche français ou étrangers, des laboratoires publics ou privés.

Stochastic Analysis of WPT Efficiency due to Location Uncertainty of mm-Sized Deep-Implanted Pacemakers

***Abstract*—The lossy and heterogeneous nature of the body tissues and the significant wave-impedance contrast as the electromagnetic wave propagates inside the body limits the fundamentally achievable efficiency of far- and midfield wireless charging of deep-body implantable devices. In addition, fluctuations in the implant position cause a further variation in the maximum power transfer efficiency. In this work, the analyzed problem consists of a wireless charged deep-implanted pacemaker considering an electric and a magnetic radiation source and a uniform distribution of pacemaker's positions inside the heart. The results show that the optimal frequency remains the same despite the position fluctuations. However, the efficiency bounds are strongly related to the nature of the source. Therefore, the proposed model and the obtained results serve as a gauge for designing implantable wireless power transfer systems and predicting variations in their efficiency.**

***Index Terms*—bioelectronics, efficiency bounds, implantable devices, pacemaker, wireless power transfer.**

I. Introduction

Implantable bioelectronics emerges as an outstanding advance in medicine, enabling innovative approaches from diagnostics to treatments. Furthermore, the application of wireless power transfer techniques to these devices extends their potential applications and enables significant miniaturization of these implants. For instance, inductive wireless charging techniques have been used for powering sub-cutaneous pacemakers [1], [2], whereas powering the ones deep-implanted in the heart requires the application of far- and midfield approaches [3], [4].

However, further analysis of the electromagnetic wave energy transfer between the on-body transmitter and the implantable receiver is required to establish the efficiency limits and ensure compliance with the safety requirements. In order to determine the efficiency bounds on the power radiated by implantable devices, different approaches have been proposed in the literature. Most of them consist of stratified models with simplified geometry, in general planar [5] or spherical [6]–[8]. These models predict the maximum theoretical efficiency and the optimal frequency and quantitatively describe the loss mechanism in these systems. The simplified models lead to more generalized results; however, they cannot represent the complexities of the body structures. For this reason, some studies employ anatomical models [9], [10] in their analysis when determining the maximum efficiency in a particular application is envisaged.

In this work, the problem of wirelessly charging a deep-implanted pacemaker is modeled based on a two-dimensional anatomical model of the human pectoral. Based on this model, the maximum achievable efficiency and the optimal frequency are calculated considering an electric and a magnetic transmitter, and their performance is compared. Besides, this model is used to evaluate the sensitivity of these efficiency bounds to the unceasing fluctuations in the implant positions caused by the heart movements. Therefore, the results described in this work can help design wireless powered deep-implanted pacemakers and predict their charging efficiency.

II. Problem Formulation

In order to analyze the efficiency bounds on wireless powering a pacemaker implanted directly in the human myocardium, the problem is geometrically represented through a two-dimensional cross-section of the pectoral region, as shown in Fig. 1(a). In this model, the closed regions representing the human organs are filled by dielectrics with equivalent complex permittivities as established in [11]. Furthermore, the transmitter and receiver are assumed to be perfectly aligned along the $\widehat{\mathbf{z}}-$ (out-of-plane) axis. Therefore, the translational invariance is justified, and the problem can be treated as two-dimensional.

As indicated in Fig. 1(a), the receiver is represented as a lossless circular region with radius $R = 1$ mm, filled by a dielectric with its real permittivity matched to the heart. In addition, the on-body transmitter is considered to surround the entire body surface representing the best-case scenario and therefore allowing to evaluate the fundamental efficiency bounds. In order to minimize the losses due to reflection at the interface between the body and external medium, the latter is filled by the same dielectric constant as the skin and zero conductivity.

Considering that the media composing the organs are linear and disregarding polarization mismatching, the reciprocal problem can be analyzed [12]. Therefore, for calculation purposes, the radiation source is considered inside the circular domain Ω_s, whereas the received power is evaluated over the on-body surface Ω_p. In this way, based on the time-harmonic electric $\mathbf{E}$ and magnetic $\mathbf{H}$ fields, the transmitted P_t, received P_r, and dissipated power P_d can be calculated through the integrals (1a)-(1c) below:

This study was supported in part by ANR "MedWave" project and in part by the *Région Bretagne* through the project SAD "EM-NEURO".

$$P_t = \oint_{\Omega_s} \left(\frac{1}{2}\mathbf{E} \times \mathbf{H}^*\right) \cdot \mathrm{ds}, \tag{1a}$$

$$P_r = \oint_{\Omega_p} \left(\frac{1}{2}\mathbf{E} \times \mathbf{H}^*\right) \cdot \mathrm{ds}, \tag{1b}$$

$$P_d = \frac{1}{2}\int_{\Omega_p} \sigma \left|\mathbf{E}\right|^2 \, \mathrm{d}v. \tag{1c}$$

So that the energy is conserved as follows [12]:

$$P_t = P_r + P_d + i2\omega(\overline{W_m} - \overline{W_e}), \tag{2}$$

where $\overline{W_m}$ and $\overline{W_e}$ are the time-averaged energies stored in the magnetic and electric fields, respectively.

From the real parts of the transmitted $\Re(P_t)$ and received $\Re(P_r)$ powers, the wireless power transfer efficiency η can be defined as:

$$\eta \equiv \frac{\Re(P_r)}{\Re(P_t)}. \tag{3}$$

Disregarding the impedance mismatch between the antennas and the electronic circuits connected to them as well as other system-level losses in these same circuits, the losses in an implantable wireless power transfer system are mainly due to the wave attenuation in the lossy body tissues. In addition, reflections at the interface body-transmitter, the heart-receiver, and between the inner organs reduce the power delivered to the receiver. While the reflection at the two first interfaces can be mitigated by adequately designing the transmitter and receiver (e.g., by employing high-permittivity and low-loss substrates [13] matched to the wave impedance at the skin and the heart, respectively), the losses due to attenuation and reflection at the transition between organs are unavoidable. Therefore, the way the problem is defined in this work assures that the calculated efficiency is limited only by the inexorable loss sources, so the following results characterize the efficiency bounds in the wireless charging efficiency for deep-implanted pacemakers.

III. Method of Analysis

The electromagnetic field and integrals (2a) and (2b) were numerically evaluated using the 2D full-wave simulation module implemented in the simulation suite COMSOL Multiphysics with the geometric representation shown in Fig. 1(a) and described in the previous section.

This work considers two radiation sources, an electric and a magnetic, as shown in Figures 1(b) and 1(c). These sources are modeled as point dipoles located at the center of the receiver's encapsulation with electric dipole moment vector $\mathbf{n_p^E} = 1\ A \cdot m\,\hat{\mathbf{x}}$ and magnetic dipole moment vector $\mathbf{n_p^H} = 1\ A \cdot m^2\,\hat{\mathbf{x}}$. These vectors were assigned as $\hat{\mathbf{x}}$-oriented once in this direction, the radiation pattern is parallel to the chest boundary, in which the on-body region is the closest to the source. Consequently, this orientation maximizes the integral (1b).

Finally, in order to evaluate the effect of the implant positioning on the efficiency bounds, this simulation was performed with 200 uniformly distributed random positions inside the heart, such as represented in Fig. 1(a) by the gray circles.

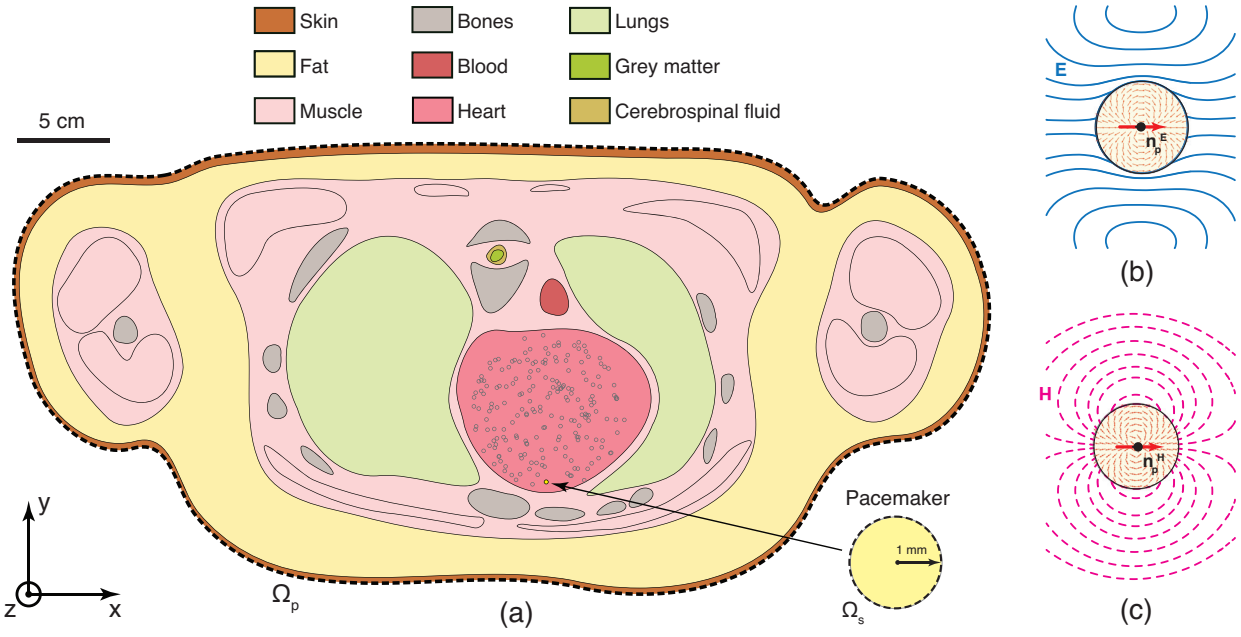


Fig. 1. Proposed formulation for evaluating the efficiency bounds of wirelessly charging a deep-tissue pacemaker: (a) Anatomical two-dimensional model of a human pectoral region comprising nine lossy tissues. The transmitter is an on-body source that covers the entire body surface whereas the receiver is a pacemaker implanted inside the myocardium. The evaluated implanted positions are represented by the gray circles. The sources are modelled as an (b) electric and (c) magnetic point dipole with moment vectors $\mathbf{n_p^E}$ and $\mathbf{n_p^H}$, respectively. Their corresponding electric $\mathbf{E}$ (continuous blue line) and magnetic $\mathbf{H}$ (dashed pink line) fields are also indicated.

IV. Results

First, it is important to validate the assumptions that the reflections at the interface between the heart-receiver and the body-transmitter can be disregarded in this proposed model. The first case is justified as the receiver is located inside the heart, and its size is much smaller than the heart size. However, once the on-body transmitter occupies a larger surface, the reflections at the interface body and external medium are more significant. Besides, in this work, the external medium is filled by a lossless dielectric perfectly matched to the wave impedance in the skin. It can also be argued that the other tissues will change the effective permittivity, affecting the wave impedance inside the body.

For this validation, the reflection coefficient at the transition between two media is defined as:

$$\Gamma \equiv \frac{Z_1 - Z_2}{Z_1 + Z_2}, \tag{4}$$

where Z_1 and Z_2 are respectively the wave impedance in the medium 1 (inside the body) and 2 (external medium), which can be calculated as $Z_n = \sqrt{(j\omega\mu_0)/(\sigma_n + j\omega\varepsilon_n)}$, being σ_n the conductivity and ε_n the electric permittivity of the medium n.

The absolute value for the reflection coefficient over a frequency span of 10 MHz to 10 GHz is presented in Fig. 2 for a plane wave propagating at the interface between two different media considering the wave impedance in medium 1 the same as in the skin Z_{skin} and also in the effective medium formed by the nine tissues $Z_{\text{effective}}$. In contrast, the medium 2 was set as air Z_{air} or the lossless and skin-like dielectric $Z_{\text{lossless skin}}$.

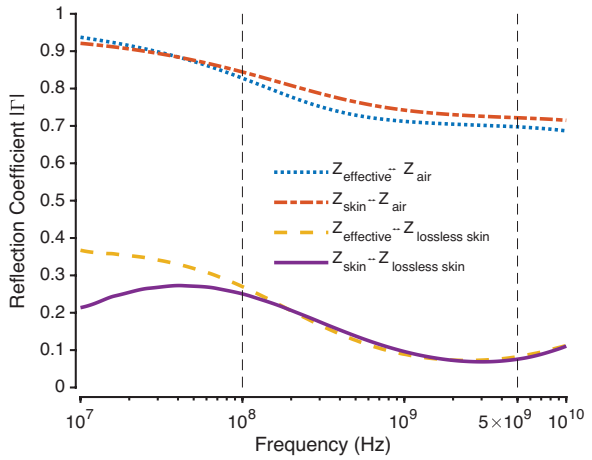


Fig. 2. Reflection coefficient for a plane wave propagating at the interface between two media for different scenarios. The wave impedance in the air is indicated as Z_{air}, in the skin as Z_{skin}, in the lossless skin as $Z_{\text{lossless skin}}$, and $Z_{\text{effective}}$ in the effective medium composed of the nine tissues present in the pectoral model.

As Fig. 2 demonstrates, there is a significant wave impedance contrast when the external medium is considered air, leading to a high reflection coefficient. Even though it decreases with the frequency, more than 70% of the transmitter power is reflected over the entire analyzed range. On the other hand, this reflection is considerably reduced when the external medium is matched to the body's wave impedance. For frequencies below 50 MHz, the electromagnetic properties of the other tissues affect the effective permittivity. Therefore, the reflection coefficient can be even twice as high if only the intrinsic impedance in this skin is considered. However, as the frequency increases matching the wave impedance in the external medium to the skin leads to a reflection coefficient numerically equivalent to matching with the effective medium. It is important to point out that the first approach is used once from the practical perspective is much easier to know the wave impedance only in the skin than experimentally characterize an effective medium. Finally, the results in Fig. 2 shows that the assumptions proposed in this work are valid over 100 MHz and, in the range between 100 MHz and 5 GHz, the reflected power is lower than 20%. For this reason, this frequency span will be considered for the following analysis.

After calculating the received power for each one of the 200 pacemaker positions indicated in Fig. 1(a), the efficiencies considering an electric and magnetic source are shown in Fig. 3(a) and 3(b), respectively. Overall, it can be noticed that a change in the receiver position inside the heart leads to a variation of the efficiency value inside a range, but the optimal frequency remains unaffected. Even though previous works have shown that the frequency in which the efficiency peaks reduces as the implantation depth increases [14], the results presented in Fig. 3 are justified once for all positions the receiver is confined in the same medium, and the implantation depth varies within a small range. Furthermore, the verified optimal frequency stability assures that these variations on the implant position cannot detune the system

The nature of the source, in turn, substantially affects the efficiency bounds. First, for an electric source, the efficiency increases with the frequency until reaching its maximum at 1.097 GHz; after that, a sharp decrease is verified. At this optimum frequency, the average efficiency is equal to 1.85×10^{-3}, but depending on the position, it goes from 9.49×10^{-4} to 5.21×10^{-3}. On the other hand, the magnetic source leads to maximum efficiency at low frequencies, and it decreases as the frequency increases. For comparison purposes, at 1.097 GHz, the average efficiency for a magnetic source is 1.03×10^{-2}, ranging from 2.91×10^{-2} to 5.05×10^{-3} with the variation on the pacemaker's position.

Once the reflections at the interface between the body and the receiver or transmitter can be disregarded and the inner reflections equally affect the performance for both sources, the factor that favors the most the magnetic source over the electric one is the fact that the body structures have low interaction with the magnetic field (note that the opposite trend can be observed for the case of implantable radiating structures [8]). In contrast, the electromagnetic field is significantly attenuated in the tissues. Such attenuation increases with the frequency, but at lower frequencies, the near field losses deteriorate the η_E. Consequently, a trade-off between these two loss causes is reached at the optimal frequency.

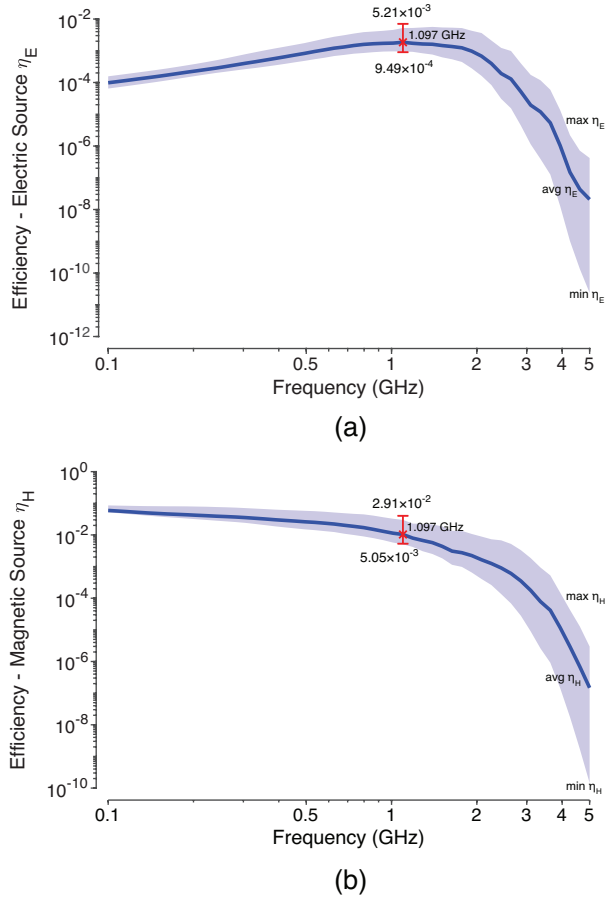


Fig. 3. Wireless power transfer efficiency for an (a) electric source and (b) magnetic source. The continuous blue line is the efficiency averaged (avg η) over the 200 evaluated receiver positions. The upper and lower limits of the blue area represent the efficiency at the position that leads to the maximum (max η) and minimum (min η) values. The red bar indicates the variation in the efficiency at the optimal frequency.

V. Conclusion

In this work, the theoretical bounds on the wireless charging efficiency of a deep-implanted pacemaker are evaluated as a function of the frequency and the implant position. First, the efficiency analysis over the frequency allows one to quantify the effect of losses on the efficiency and determine the optimal operating frequency in each case. In addition, by carrying out this analysis for many randomly distributed implant positions, it is possible to determine the variation on the maximum achievable efficiency due to fluctuations in the implantation depth.

Therefore, a model based on the two-dimensional cross-section of the human pectoral composed of nine different tissues is analyzed. Furthermore, this model is proposed so that all loss sources that could be mitigated in practical implementations are disregarded; thus, only the intrinsic losses are taken into account. In this way, the calculated efficiency corresponds to the maximum theoretical efficiency achieved in this given application.

The results obtained through this proposed model show that fluctuations in the implant position are not able to detune the system once the maximum efficiency is achieved at the same frequency for all positions. It is also shown that a magnetic radiation source monotonically decreases with the frequency, whereas an electric transmitter presents an optimum frequency at 1.097 GHz. This behavior is because there is practically no interaction between the magnetic field and the body tissues while strongly attenuating the electric field. The near field coupling reduces efficiency at lower frequencies for an electric source while the wave is almost completely attenuated at higher frequencies. Therefore, the efficiency reaches a peak at the mid-field range.

Finally, it should be stated that a specific problem of a wireless charged pacemaker is investigated in this work; however, the proposed model can also be applied to analyze wireless power transfer efficiency in different implantable devices applications. Furthermore, the obtained results can be used as a guideline to design miniaturized deep-implanted pacemakers and predict wireless charging efficiency fluctuations.

References

[1] C. Liu, C. Jiang, J. Song, and K. T. Chau, "An effective sandwiched wireless power transfer system for charging implantable cardiac pacemaker," *IEEE Trans. Ind. Electron.*, vol. 66, no. 5, p. 4108–4117, May 2019.

[2] T. Campi, S. Cruciani, F. Palandrani, V. D. Santis, A. Hirata, and M. Feliziani, "Wireless power transfer charging system for aimds and pacemakers," *IEEE Trans. Microw. Theory Tech.*, vol. 64, no. 2, p. 633–642, Feb. 2016.

[3] J. S. Ho *et al.*, "Wireless power transfer to deep-tissue microimplants," *Proc. Natl. Acad. Sci.*, vol. 111, no. 22, p. 7974–7979, Jun. 2014.

[4] H. Le-Huu and C. Seo, "Bipolar spiral midfield wireless power transfer for cardiac implants application," *IEEE Antennas Wirel. Propag. Lett.*, p. 1–1, Jun. 2021.

[5] A. S. Y. Poon, S. O'Driscoll, and T. H. Meng, "Optimal frequency for wireless power transmission into dispersive tissue," *IEEE Trans. Antennas Propag.*, vol. 58, no. 5, p. 1739–1750, May 2010.

[6] A. K. Skrivervik, M. Bosiljevac, and Z. Sipus, "Fundamental limits for implanted antennas: maximum power density reaching free space," *IEEE Trans. Antennas Propag.*, vol. 67, no. 8, p. 4978–4988, Aug. 2019.

[7] M. Gao, D. Nikolayev, M. Bosiljevac, Z. Šipuš, and A. K. Skrivervik, "Rules of thumb to assess losses of implanted antennas," in *Proc. 2021 15th European Conference on Antennas and Propagation (EuCAP)*, Mar. 2021, p. 1–5.

[8] D. Nikolayev, W. Joseph, M. Zhadobov, R. Sauleau, and L. Martens, "Optimal radiation of body-implanted capsules," *Phys. Rev. Lett.*, vol. 122, no. 10, p. 108101, Mar. 2019.

[9] D. Nikolayev, M. Zhadobov, P. Karban, and R. Sauleau, "Electromagnetic radiation efficiency of body-implanted devices," *Phys. Rev. Applied*, vol. 9, no. 2, p. 024033, Feb. 2018.

[10] I. V. Soares, R. Sauleau, and D. Nikolayev, "Theoretical analysis of electromagnetic exposure to wireless charging systems for deep-body implantable devices," in *Proc. BioEM 2021*, Sep. 2021, p. 1–3.

[11] S. Gabriel, R. W. Lau, and C. Gabriel, "The dielectric properties of biological tissues: III. Parametric models for the dielectric spectrum of tissues," *Phys. Med. Biol.*, vol. 41, no. 11, p. 2271–2293, Nov. 1996.

[12] J. D. Jackson, *Classical electrodynamics*, 3rd ed. New York: Wiley, 1999.

[13] D. Nikolayev, W. Joseph, A. K. Skrivervik, M. Zhadobov, L. Martens, and R. Sauleau, "Dielectric-loaded conformal microstrip antennas for versatile in-body applications," *IEEE Antennas Wirel. Propag. Lett.*, vol. 18, no. 12, p. 2686–2690, Dec. 2019.

[14] I. V. Soares *et al.*, "Physical bounds on implant powering efficiency using body-conformal WPT systems," in *Proc. 2021 IEEE Wireless Power Transfer Conference (WPTC)*, Jun. 2021, p. 1–4.